Activation of the endomitotic spindle assembly checkpoint and thrombocytopenia in Plk1-deficient mice

Marianna Trakala, David Partida, María Salazar-Roa, María Maroto, Paulina Wachowicz, Guillermo de Cárcer and Marcos Malumbres

Cell Division and Cancer group,

Spanish National Cancer Research Centre (CNIO), Madrid

Running title: Plk1 is essential for megakaryopoiesis

Keywords: Centrosome maturation, Endomitosis, Megakaryocyte, Platelet, Polo-like kinase 1, Polyploidization, Spindle Assembly Checkpoint.

Correspondence: M. Malumbres, Centro Nacional de Investigaciones Oncológicas (CNIO), Melchor Fernández Almagro 3, E-28029 Madrid. Tel. +34 91 732 8000; Fax +34 91 732 8033; E-mail: malumbres@cnio.es.

Key points

Plk1 ablation activates an endomitotic checkpoint in megakaryocytes

Plk1 deficiency in megakaryocytes results in thrombocytopenia

Abstract

Polyploidization in megakaryocytes is achieved by endomitosis, a specialized cell cycle in which DNA replication is followed by aberrant mitosis. Typical mitotic regulators such as Aurora kinases or Cdk1 are dispensable for megakaryocyte maturation, and inhibition of mitotic kinases may in fact promote megakaryocyte maturation. However, we show here that Polo-like kinase 1 (Plk1) is required for endomitosis and ablation of the *Plk1* gene in megakaryocytes results in defective polyploidization accompanied by mitotic arrest and cell death. Lack of Plk1 results in defective centrosome maturation and aberrant spindle pole formation, thus impairing the formation of multiple poles typically found in megakaryocytes. In these conditions, megakaryocytes arrest for a long time in mitosis and frequently die. Mitotic arrest in wild-type megakaryocytes treated with Plk1 inhibitors or Plk1-null cells is triggered by the Spindle Assembly Checkpoint (SAC), and can be rescued in the presence of SAC inhibitors. These data suggest that, despite the dispensability of proper chromosome segregation in megakaryocytes, an endomitotic SAC is activated in these cells upon Plk1 inhibition. SAC activation results in defective maturation of megakaryocytes and cell death, thus raising a note of caution in the use of Plk1 inhibitors in therapeutic strategies based on polyploidization regulators.

Introduction

Megakaryocytes are bone marrow cells specialized in the generation of platelets[1]. Once committed to differentiation, megakaryocyte progenitor cells undergo several rounds of endomitotic cell cycles in which the latest stages of mitosis are aborted to render polyploid cells. After genome duplication, megakaryocytes enter mitosis by breaking down the nuclear envelope and condensing chromosomes, but they exit mitosis in the absence of complete karyokinesis generating polylobulated nuclei[1,2]. This process is thought to be mediated by impaired furrow formation due to impaired RhoA activity and defective formation of the actomyosin ring required for cytokinesis[3,4]. The increase in ploidy is a necessary component of megakaryocyte differentiation and only high-ploidy cells are able to shed platelets efficiently. Although the reason for this requirement is not completely clear, the increase in ploidy accompanies the increase in cellular volume and this may provide cells with sufficient cytoplasmic volume to generate a large number of platelets[1,5,6].

Since mitosis is aborted in its later stages, the requirement for mitotic regulators during megakaryocyte polyploidization has been a matter of debate. Earlier work in cell lines suggested defective activity of mitotic cyclins and its catalytic partner cyclin-dependent kinases (Cdk1)[reviewed in Ref. 5]. Recent expression data indicate that the mitotic machinery is normally expressed in megakaryocytes whereas it is downregulated in endocycling cells, i.e. cells that polyploidize through successive cycles in the complete absence of mitotic features such as trophoblast giant cells[7]. Yet, although specific mitotic kinases such as Aurora A or Aurora B or its partners are

expressed in megakaryocytes, they are dispensable for polyploidization or maturation of these cells[8-13].

Plk1 is a member of the Plk family involved in centrosome maturation, formation of the mitotic spindle, microtubule-chromosome attachment, as well in cytokinesis[14-17]. Similarly to Aurora A inhibition, inhibition of Plk1 results in defective centrosome maturation and spindle formation. Due to its critical functions in the mitotic cell cycle and its expression in human tumors, Plk1 has been proposed as a cancer target and recent clinical trials with Plk1 inhibitors have indeed shown significant therapeutic effect in hematopoietic tumors[15,18-21]. These findings have been used to propose new therapeutic strategies based on the idea that inhibition of mitotic kinases, including members of the Cdk, Aurora or Polo-like kinase (Plk) family, should impair growth of leukemia [e.g. acute megakaryocytic leukemia (AMKL)] cells without affecting polyploidization or function of normal megakaryocytes[9,22], a feature that could protect patients from thrombocytopenia, a major side effect of anti-proliferative therapies.

To understand the relevance of Plk1 during megakaryocyte differentiation we have analyzed the effect of the specific genetic ablation of the murine Plk1 locus using a new conditional knockout model recently generated in our laboratory. Contrary to the inhibition of Aurora kinases, elimination of Plk1 results in strong defects in megakaryocyte maturation in vivo. Plk1 deficiency prevents megakaryocyte polyploidization as a result of the activation of the Spindle Assembly Checkpoint (SAC) in these cells. This results in prolonged mitotic arrest and death of Plk1-null megakaryoyctes resulting in severe thrombocytopenia in vivo. These data highlight the functional relevance of the SAC in endomitotic megakaryocytes and add a note of caution in the general use of mitotic kinase inhibitors in therapeutic strategies based on polyploidization regulators.

Materials and Methods

Mouse models and histopathological analysis. A 0.8-kb fragment containing the murine *Plk1* exon 2 was flanked with loxP sites and followed by a PGK-neomycin phosphotransferase (neo) cassette, flanked by frt sites, for positive selection of ES cell clones. Recombinant clones were selected by southern blot and the neo cassette was removed using Flp recombinase to generate the Plk1 conditional allele [*Plk1*(lox)] (P.W. and G.d.C., submitted for publication). Pf4-Cre mice and the megakaryocyte-specific Cdc20 conditional knockout were described previously[12,23]. All animals were maintained in a mixed 129/Sv (25%) times CD1 (25%) times C57BL/6J (50%) background. Mice were housed in the pathogen-free animal facility of the Centro Nacional de Investigaciones Oncológicas (CNIO, Madrid) following the animal care standards of the institution. All animal protocols were approved by the local committee for animal care and research. Thrombopoietin (TPO 1.2 μg/mouse) was injected subcutaneously into 8-12-week-old mice and platelet counts were analyzed 4 days later. The following antibodies were used for immunohistochemistry in tissue sections: Von Willebrand Factor (FVIII, Dako; 1:2000), phospho-histone H3 (Ser10; Millipore; 1:2000) or Plk1 (new monoclonal antibody generated in our lab; unpublished data). For quantification, paraffin sections stained with anti-VWF were examined using an Olympus BX51 microscope equipped with objective lenses (40/0.75, 20/0.4, 10/0.25, and 4/0.1). The relative amount of pixels positive for VWF was used as a score.

Flow Cytometry. Flow cytometric analysis of DNA content and surface markers of megakaryocytes was determined by staining either whole bone marrow cells or hematopoietic progenitor cultures from 0-5 days in presence of TPO with fluorescein isothiocyanate (FITC)–conjugated anti-CD41 antibody (BD Biosciences) followed by

fixation with 4% PFA at room temperature for 30 min followed by staining with 2 μg/ml DAPI (4,6 diaminophenylindole, Sigma-Aldrich).

Immunofluorescence. Lin$^-$ bone marrow cells were grown in Dulbecco's modified Eagle's medium (DMEM; Gibco) supplemented with antibiotics and 10% fetal bovine serum (FBS), and stimulated with 50-100 ng/mL murine TPO (PeproTech) until cells were harvested for analysis (three days unless indicated otherwise). For immunofluorescence, cells were fixed with 4% paraformaldehyde in PBS for 10 min at 37ºC, permeabilized with PBS-Triton 0.15% for 2 min at 37ºC, blocked with 3% BSA and subsequently incubated during 1-3 h with the primary antibody against Plk1 (unpublished data), pericentrin (Abcam 4448), Bub1 (a gift from Stephen Taylor), Mad2 (a gift from Katja Wassmann), α-tubulin (Sigma), phospho-histone H3 (pH3; Millipore 06-570). Anti-centromere antibodies (ACA; Antibodies Incorporated 15-235) were used to stain centromeres and fluorescent-conjugated-phalloidin (Sigma) was used to stain actin fibers. Matching secondary antibodies with different Alexa dies (488, 555, 594, 647; Molecular Probes) and DAPI (Prolong Gold antifade; Invitrogen) were used for nuclei visualization. Image acquisition was performed using either a confocal ultra-spectral microscope (Leica TCS-SP5) or a Leica DMI fluorescence 6000B microscope. In these assays, Taxol was used at 300 nM, the Plk1 inhibitor BI2536 at 100nM, and reversine was used at 1 μM for inhibition of the SAC kinase Mps1 [24].

Time-lapse microscopy. Cells were transduced with lentiviruses or retroviruses encoding histone H2B-GFP, lamin A-CFP (a gift from V. Andrés, CNIC, Madrid) and geminin-mCherry as reported previously[12]. Transduced cells were then plated on eight-well glass-bottom dishes (Ibidi) embedded in methylcellulose (MethoCult M3231; Stem

Cell Technologies) mixed 1:1 with Iscove's Modified Dulbecco's Medium (IMDM) containing 4% Fetal Bovine Serum and 100 ng/mL murine TPO, in order to minimize cell movement. Time-lapse acquisition was performed with a Leica DMI 6000B microscope equipped with a 63×/1.5 N.A. objective lens or DeltaVision RT imaging system (Applied Precision; IX70/71; Olympus) equipped with a Plan Apochromatic 40×/1.42 N.A. objective lens, and maintained at 37 °C in a humidified CO2 chamber. Images were acquired every 7 min for up to 10 days. Quantitative analysis was performed by ImageJ software.

Transmission electron microscopy. Cells were fixed for 3 hours at room temperature in 3% glutaraldehyde (v/v) in 0.4 M HEPES buffer pH 7.4, washed and fixed again in aqueous 1% (w/v) osmium tetroxide, and embedded in Epon. Electron microscopy was performed with a JEOL 1230 transmission electron microscope, at 80 kV, on ultra-thin sections of 60 nm.

Statistical analysis. Statistical analysis was carried out using Prism 5 (GraphPad). All statistical tests were performed using two-sided, unpaired Student's t-tests. Data with $p < 0.05$ were considered statistically significant. In most figures, *, $p<0.05$; **, $p<0.01$; ***, $p<0.001$.

Results

Lack of Plk1 results in impaired megakaryocyte maturation

To specifically eliminate Plk1 in megakaryocytes we made use of a Plk1 conditional allele [*Plk1*(lox)], recently generated in our laboratory (see Methods), and Pf4-Cre transgenic mice in which the Cre recombinase is expressed under Platelet factor 4 regulatory transcriptional sequences leading to efficient recombination in medium and high-ploidy megakaryocytes[23],[12]. Cre activity in *Plk1*(lox/lox) mice results in genetic ablation of Plk1 exon 2 generating *Plk1*(Δ/Δ) mice with specific ablation of Plk1 in megakaryocytes. Plk1 was absent in mitotic megakaryocytes from *Plk1*(Δ/Δ) mice but was strongly expressed in control littermates (Figure 1a) or in Cdc20-deficient megakaryocytes[12], which are arrested in mitosis as a consequence of inactivation of the Anaphase-promoting complex/cyclosome (APC/C; Figure S1). Histopathological analysis of bone marrow sections from 8-week-old *Plk1*(Δ/Δ) mice indicated the presence of smaller megakaryocytes in which the amount of Von Willebrand Factor (VWF), a marker of megakaryocyte differentiation, was significantly reduced (Figure 1a,b). In addition, these mutant bone marrows (Figure 1c), as well as *Plk1*(Δ/Δ) spleens (Figure S2), were characterized by the presence of abundant mitotically arrested megakaryocytes, as detected after staining with antibodies against phosphorylated histone H3 (pH3). Mitotic megakaryocytes in Plk1-deficient mice frequently presented condensed chromosomes (pH3-positive) forming typical ring-structures (Figure 1d). Careful analysis of these sections revealed that megakaryocyte nuclei frequently displayed lower complexity compared to control megakaryocytes from control littermates, with a high percentage of mononucleated or binucleated megakaryocytes

compared to complex polylobulated megakaryocytes typical of control bone marrows (Figure 1a,c,e).

To check the effect of Plk1 ablation in megakaryocyte ploidy, bone marrow cells were isolated and their DNA content was analyzed by flow cytometry. As shown in Figure 2a, lack of Plk1 resulted in defective ploidy profiles in these CD41+ cells. Whereas control cells frequently reach 16C or 32C ploidy levels, *Plk1*(Δ/Δ) megakaryocytes displayed reduced ratio of these peaks when compared to low-ploidy (4C-8C) megakaryocytes (Figure 2b). As a control, we also analyzed megakaryocytes deficient in Cdc20, a model with reduced ploidy and severe thrombocytopenia[12]. It is important to highlight that, since Plk1-, as well as Cdc20-, deficient megakaryocytes frequently accumulated as mitotic cells, these peaks at least partially represent mitotic cells (i.e. 16C peaks are likely a combination of interphasic 16C cells plus mitotic 8C cells; Figure 2a,b). Plk1 deficiency resulted in increased levels of megakaryocyte progenitors (CD41+CD42^{-} cells), as reported for Cdc20-deficient mice[12], but reduced ratio of CD41+CD42+ double positive cells suggesting defective maturation (Figure S3). In agreement with these observations, *Plk1*(Δ/Δ) mice displayed a significant decrease of circulating platelets in peripheral blood (Figure 2c), suggesting that Plk1 ablation resulted in significant levels of thrombocytopenia in these mice. Platelet morphology or size was not altered in the absence of Plk1 (Figure S4). *Plk1*(Δ/Δ) mice were however resistant to treatment with TPO suggesting a defect in the process that leads to the generation of platelets from megakaryocyte progenitors (Figure S4).

Defective mitotic exit in the absence of Plk1

To better follow megakaryocyte polyploidization, we monitored megakaryocyte maturation using time-lapse microscopy in Lin^{-} bone marrow cells after treatment with

TPO. Bone marrow progenitors were transduced with lentiviral vectors expressing green fluorescent protein (GFP)-tagged histone H2B and mCherry fluorescent protein-tagged geminin[25]. Cell cycle progression in control megakaryocytes can be monitored by levels of geminin, which is low in G1 and high in S-phase-G2-M, and the pattern of histone which allows following chromosome condensation in mitosis (Figure 3a). Since geminin is exclusively nuclear during interphase, endomitosis can also be detected by pan-cellular localization of geminin in these cells as a consequence of nuclear envelope breakdown[12]. In the absence of Plk1, cells entered normally into mitosis; i.e. chromosomes condensed and geminin signal was pan-cellular due to the absence of nuclear envelope. However, geminin signal remained high for more than 20 h during mitosis (chromosomes condensed and pan-cellular signal of geminin) until cells died (Figure 3b). In a few cases, *Plk1*(Δ/Δ) megakaryocytes were able to exit from mitosis but they usually died in the following interphase before they were able to start a new cycle of geminin expression (Figure 3b,c). Whether this death is a direct consequence of Plk1 ablation or is partially due to the intense manipulation of these cultured megakaryocytes is not clear at present. On average, Plk1-deficient megakaryocytes spent about 30 h in mitosis, whereas the duration of mitosis in normal megakaryocytes was 57 ± 14 min (Figure 3d). Interestingly, this arrest in mitosis was even longer than the one obtained after genetic ablation of Cdc20, a model in which mitotic exit is prevented leading to metaphase arrest for long periods of time until they die[12,26].

Lack of Plk1 results in defective centrosome maturation and abnormal spindle formation in megakaryocytes

Three days after stimulation with TPO, *Plk1*(Δ/Δ) $CD41^+$ cells displayed reduced polyploidization (Figure 4a) similarly to what was observed in bone marrow cells

(Figure 2a). In addition, the percentage of $CD41^+$ cells was enhanced both in *Plk1*(Δ/Δ) and *Cdc20*(Δ/Δ) cultures mainly due to the increase in low complexity $CD41^+$ cells (Figure S3). These defects were also accompanied by a significant accumulation of mitotic cells as detected by CD41 (not shown) and Giemsa staining (Figure 4b). As in other mitotic cells, Plk1 displayed a diffused localization in control megakaryocytes with some concentration at kinetochores and strong centrosomal signal (Figure 4c). Plk1 immunoreactivity was lost in *Plk1*(Δ/Δ) megakaryocytes which were characterized by abnormal distribution of mitotic chromosomes frequently forming ring-like structures (Figure 4c-d). These structures were likely a consequence of defective centrosomal maturation and the presence of collapsed spindle poles (Figure 4e). In fact, the staining for pericentrin at centrosomes, a marker of mature organelles, was significantly reduced in Plk1-deficient megakaryocytes (Figure 4e,f). In some cases, pericentrin signals were concentrated in a reduced area forming a single spindle pole, whereas in other cases, microtubule asters emanated from weak or absent pericentrin marks (Figure S5). The number of spindle poles was also reduced indicating lack of centrosome separation or centrosome collapse into a single or a few poles around which chromosomes organized into ring structures (Figure 4e and Figure S5). As a comparison, mitotic arrest induced by taxol did not result in decreased pericentrin staining or reduced number of poles (Figure 4e,f). Transient inhibition of Plk1 with the small-molecule compound BI2536 during 12 h in control cells resulted in similar phenotypes to those observed in the genetic model (Figure 4e,f), suggesting that these defects were a consequence of specific loss of Plk1 activity in megakaryocytes.

Lack or inhibition of Plk1 results in a SAC-dependent mitotic arrest

The defects in centrosome maturation and spindle structure suggested that mitotic arrest in Plk1-deficient megakaryocytes could be a consequence of an active SAC. This mitotic checkpoint has been shown to be present in megakaryocytes using Cdc20 as an indirect readout[27], although its relevance has not been established given the lack of genome segregation into separate cells. We therefore monitored the presence of two bona-fide SAC proteins, Bub1 and Mad2, in Plk1-deficient megakaryocytes or control cultures. *Plk1*(Δ/Δ) megakaryocytes or *Plk1*(lox/lox) cells treated with the Plk1 inhibitor BI2536 displayed a significant accumulation of the SAC components Bub1 (Figure 5a) and Mad2 (Figure 5b) at the kinetochores as detected using anti-centromeric antibodies (ACA), similarly to control cells treated with taxol, suggesting the presence of an active SAC. As a negative control we used Cdc20-deficient megakaryocytes, in which the mitotic arrest is known to occur once the SAC has been satisfied and it is therefore SAC-independent[26].

To finally analyze whether this checkpoint was responsible for the mitotic arrest in cells with defective Plk1 function, we use reversine, a small-molecule inhibitor of the SAC kinase Mps1 [24]. Reversine was able to significantly rescue the accumulation of mitotic cells in *Plk1*(Δ/Δ) cultures, as well as in *Plk1*(lox/lox) cells treated with BI2536 or taxol (Figure 6a-c and Figure S6). In Plk1-deficient cells or in the presence of BI2536, reversine induced mitotic exit giving rise to cells with interphasic ring nuclei or in which chromosomes formed multiple curved nuclei around the collapsed spindles (Figure 6a,b). Reversine, however, had no effect in the mitotic arrest imposed by the lack of Cdc20 (Figure 6b,c), a defect known to be SAC independent[26]. All together, these observations support the notion that lack of Plk1 prevents mitotic progression and megakaryocyte polyploidization by triggering a SAC-dependent response.

Discussion

The intrinsic differences between mitotic and endomitotic cell cycles have raised the possibility of using mitotic kinase inhibitors for treating hematological malignancies such as pro-megakaryocytic leukemias[22]. Many mitotic kinases such as Aurora A, Aurora B, Cdk1 or Plk1 are essential for the mitotic cell cycles and their genetic ablation results in lack of cell division in the embryo, most somatic cells and tumor cells[13,15,17,28-30]. Yet, inhibition or genetic ablation of Aurora A or Aurora B does not perturb megakaryocyte polyploidization or maturation[9,11-13]. In addition, Cdk1 deficiency results in an alternative polyploidization mechanism based on endocycling that has no major effects in platelet production[12]. In this manuscript, we report that contrary to these other mitotic kinases Plk1 is essential for megakaryocyte polyploidization and its ablation results in thrombocytopenia.

Endomitotic megakaryocytes are characterized by the presence of multipolar spindles with an asymmetrical distribution of chromosomes. Early studies in cell lines suggested that megakaryocytes can polyploidize in the presence of antimicrotubule poisons, suggesting the irrelevance of the SAC in these cells[31]. More recent data, however, showed that nocodazole arrests primary megakaryocytes in the presence of Cdc20 signal at the kinetochores indicating that the SAC may be activated in these cells in the presence of microtubule poisons[27,32,33]. Sister chromatid separation seems to occur asymmetrically towards the different poles, and chromosomes cluster into a ring around each aster suggesting that each chromosome ring may give rise to one lobe of the megakaryocytic nucleus[27]. The asymmetric segregation of chromosomes towards the multiple poles suggested that the SAC is permissive for the complex attachment of chromosomes to multipolar spindles in megakaryocytes[27]. That situation is altered in Plk1-deficient megakaryocytes, likely as a consequence of the formation of monopolar

spindles that prevent proper attachment of chromosomes. In the absence of Plk1, all chromosomes are forming a single or a few rings around the only or the few poles present, in agreement with the presence of megakaryocytes with a single or fewer lobules in vivo (see model in Figure S5). These defects in spindle formation likely lead to a checkpoint-dependent mitotic arrest that in most cases triggers cell death, showing that megakaryocytes can also monitor defects in spindle assembly using a functional SAC. The complexity of endomitosis likely requires multiple other pathways, in addition to the Plk1-SAC axis, to generate functional polyploid megakaryocytes with multilobulated nuclei. Yet, the similarities and differences between mitotic and endomitotic cell cycles remain mostly unknown.

The SAC is a complex network that inhibits the APC/C-Cdc20 activity, thus preventing securin and cyclin B degradation and delaying mitotic exit, in the presence of unattached kinetochores[34]. Yet, cells can be able to exit from mitosis even in the presence of an unsatisfied SAC due to a process known as mitotic slippage[35]. During this process, cyclin B1 is slowly degraded as a consequence of weak APC/C-Cdc20 activity and, in fact, mitotic slippage does not occur in Cdc20-null cells and cells arrest in mitosis until they die[26]. The fact that Plk1-deficient megakaryocytes arrest in mitosis for longer periods of time than Cdc20-deficient megakaryocytes before they die (Figure 3) suggests that Cdc20 and Plk1 may have separate implications in the mechanisms that modulate cell death in mitosis. Indeed, Cdc20 is known to suppress apoptosis through targeting Bim for degradation, suggesting increased mitotic apoptosis in the absence of this APC/C cofactor[36]. It has also been recently reported that Plk1-dependent phosphorylation of caspase-8 may trigger the extrinsic apoptotic pathway during mitosis[37]. However, treatment of Cdc20-null cells with Plk1 inhibitors does not prolong survival during mitotic arrest (data not shown) and mitotic cell death has been proposed

to be mostly mediated by the intrinsic apoptotic pathway[38]. Whether Plk1 may directly modulate cell death in megakaryocytes is unclear at present. Yet, thrombocytopenia is less dramatic in Plk1- compared to Cdc20-mutant models, likely as a consequence of the ability of some Plk1 megakaryocytes to exit from the mitotic arrest and reach higher ploidy levels.

Owing to the essential role of Plk1 in the control of the cell cycle, Plk1 is considered as an attractive cancer target with some small-molecule inhibitors showing encouraging results in clinical trials[19,20]. Volasertib (a BI2536 derivative also known as BI6727) has shown a significant effect in acute myeloid leukemia (AML) patients[39], an effect that recently received a Breakthrough Therapy designation by the FDA promoting its evaluation in Phase III clinical trials. Volasertib has also been tested in clinical trials in solid malignancies, in which the most common dose-limiting effects are thrombocytopenia and neutropenia[40,41]. These problems may be due to specific effects in progenitors cells or to the fact that Plk1 inhibitors can inhibit other kinases at specific doses[42,43]. However, our conditional knockout model suggests that Plk1 inhibition actually leads to defective polyploidization and cell death in megakaryocytes, a result with implications in the design of therapeutic protocols targeting this mitotic kinase.

Acknowledgements

We are fully indebted to V. Andrés (CNIC, Madrid, Spain) and A. Miyawaki (RIKEN, Saitama, Japan) for reagents. We thank Lola Martínez and Diego Megías (CNIO) for help with cytometry and microscopy analysis, Fernando Escobar and Begoña Pou (CIB, Madird, Spain) for help in the preparation and analysis of EM samples, members of the Comparative Pathology and Transgenic Units of the CNIO for excellent technical support, and Sara Leceta and Sheila Rueda for help with animal management. M.T.

received a fellowship from the Foundation La Caixa. The Cell Division and Cancer group of the CNIO is funded by the MINECO (SAF2012-38215), Consolider-Ingenio 2010 Programme (SAF2014-57791-REDC), Red Temática CellSYS (BFU2014-52125-REDT), Comunidad de Madrid (OncoCycle Programme; S2010/BMD-2470), Worldwide Cancer Research (WCR #15-0278) and the MitoSys project (HEALTH-F5-2010-241548; European Union Seventh Framework Programme).

Authorship Contributions

M.T. generated the mouse models, performed the experiments and analyzed the data. D.P., M.S.-R., G.d.C. and M.Maroto contributed to cellular studies. P.W. generated the Plk1 conditional allele. M.Malumbres designed and supervised the project, analyzed the data and wrote the manuscript.

Disclosure of Conflicts of Interest

The authors declare no conflicts of interests to disclose.

References

1. Kaushansky K. Historical review: megakaryopoiesis and thrombopoiesis. *Blood*. 2008;111(3):981-986.
2. Ravid K, Lu J, Zimmet JM, Jones MR. Roads to polyploidy: the megakaryocyte example. *J Cell Physiol*. 2002;190(1):7-20.
3. Lordier L, Jalil A, Aurade F, et al. Megakaryocyte endomitosis is a failure of late cytokinesis related to defects in the contractile ring and Rho/Rock signaling. *Blood*. 2008;112(8):3164-3174.
4. Gao Y, Smith E, Ker E, et al. Role of RhoA-specific guanine exchange factors in regulation of endomitosis in megakaryocytes. *Dev Cell*. 2012;22(3):573-584.
5. Zimmet J, Ravid K. Polyploidy: occurrence in nature, mechanisms, and significance for the megakaryocyte-platelet system. *Exp Hematol*. 2000;28(1):3-16.
6. Machlus KR, Thon JN, Italiano JE, Jr. Interpreting the developmental dance of the megakaryocyte: a review of the cellular and molecular processes mediating platelet formation. *Br J Haematol*. 2014;165(2):227-236.
7. Sher N, Von Stetina JR, Bell GW, Matsuura S, Ravid K, Orr-Weaver TL. Fundamental differences in endoreplication in mammals and Drosophila revealed by analysis of endocycling and endomitotic cells. *Proc Natl Acad Sci U S A*. 2013;110(23):9368-9373.
8. Geddis AE, Kaushansky K. Megakaryocytes express functional Aurora-B kinase in endomitosis. *Blood*. 2004;104(4):1017-1024.
9. Wen Q, Goldenson B, Silver SJ, et al. Identification of regulators of polyploidization presents therapeutic targets for treatment of AMKL. *Cell*. 2012;150(3):575-589.
10. Wen Q, Leung C, Huang Z, et al. Survivin is not required for the endomitotic cell cycle of megakaryocytes. *Blood*. 2009;114(1):153-156.
11. Lordier L, Chang Y, Jalil A, et al. Aurora B is dispensable for megakaryocyte polyploidization, but contributes to the endomitotic process. *Blood*. 2010;116(13):2345-2355.
12. Trakala M, Rodriguez-Acebes S, Maroto M, et al. Functional reprogramming of polyploidization in megakaryocytes. *Dev Cell*. 2015;32(2):155-167.
13. Goldenson B, Kirsammer G, Stankiewicz MJ, Wen QJ, Crispino JD. Aurora kinase A is required for hematopoiesis, but is dispensable for murine megakaryocyte endomitosis and differentiation. *Blood*. 2015.
14. Archambault V, Glover DM. Polo-like kinases: conservation and divergence in their functions and regulation. *Nat Rev Mol Cell Biol*. 2009;10(4):265-275.
15. Lens SM, Voest EE, Medema RH. Shared and separate functions of polo-like kinases and aurora kinases in cancer. *Nat Rev Cancer*. 2010;10(12):825-841.
16. de Carcer G, Manning G, Malumbres M. From Plk1 to Plk5: functional evolution of polo-like kinases. *Cell Cycle*. 2011;10(14):2255-2262.
17. Malumbres M. Physiological relevance of cell cycle kinases. *Physiol Rev*. 2011;91(3):973-1007.
18. Maire V, Nemati F, Richardson M, et al. Polo-like kinase 1: a potential therapeutic option in combination with conventional chemotherapy for the

management of patients with triple-negative breast cancer. *Cancer Res*. 2013;73(2):813-823.
19. Gjertsen BT, Schoffski P. Discovery and development of the Polo-like kinase inhibitor volasertib in cancer therapy. *Leukemia*. 2014.
20. Craig SN, Wyatt MD, McInnes C. Current assessment of polo-like kinases as anti-tumor drug targets. *Expert Opin Drug Discov*. 2014;9(7):773-789.
21. Bruinsma W, Raaijmakers JA, Medema RH. Switching Polo-like kinase-1 on and off in time and space. *Trends Biochem Sci*. 2012;37(12):534-542.
22. Krause DS, Crispino JD. Molecular pathways: induction of polyploidy as a novel differentiation therapy for leukemia. *Clin Cancer Res*. 2013;19(22):6084-6088.
23. Tiedt R, Schomber T, Hao-Shen H, Skoda RC. Pf4-Cre transgenic mice allow the generation of lineage-restricted gene knockouts for studying megakaryocyte and platelet function in vivo. *Blood*. 2007;109(4):1503-1506.
24. Santaguida S, Tighe A, D'Alise AM, Taylor SS, Musacchio A. Dissecting the role of MPS1 in chromosome biorientation and the spindle checkpoint through the small molecule inhibitor reversine. *J Cell Biol*. 2010;190(1):73-87.
25. Sakaue-Sawano A, Hoshida T, Yo M, et al. Visualizing developmentally programmed endoreplication in mammals using ubiquitin oscillators. *Development*. 2013;140(22):4624-4632.
26. Manchado E, Guillamot M, de Carcer G, et al. Targeting mitotic exit leads to tumor regression in vivo: Modulation by Cdk1, Mastl, and the PP2A/B55alpha,delta phosphatase. *Cancer Cell*. 2010;18(6):641-654.
27. Roy L, Coullin P, Vitrat N, et al. Asymmetrical segregation of chromosomes with a normal metaphase/anaphase checkpoint in polyploid megakaryocytes. *Blood*. 2001;97(8):2238-2247.
28. Fernandez-Miranda G, Trakala M, Martin J, et al. Genetic disruption of aurora B uncovers an essential role for aurora C during early mammalian development. *Development*. 2011;138(13):2661-2672.
29. Perez de Castro I, Aguirre-Portoles C, Fernandez-Miranda G, et al. Requirements for Aurora-A in tissue regeneration and tumor development in adult mammals. *Cancer Res*. 2013;73(22):6804-6815.
30. Santamaria D, Barriere C, Cerqueira A, et al. Cdk1 is sufficient to drive the mammalian cell cycle. *Nature*. 2007;448(7155):811-815.
31. van der Loo B, Hong Y, Hancock V, Martin JF, Erusalimsky JD. Antimicrotubule agents induce polyploidization of human leukaemic cell lines with megakaryocytic features. *Eur J Clin Invest*. 1993;23(10):621-629.
32. Nagata Y, Muro Y, Todokoro K. Thrombopoietin-induced polyploidization of bone marrow megakaryocytes is due to a unique regulatory mechanism in late mitosis. *J Cell Biol*. 1997;139(2):449-457.
33. Vitrat N, Cohen-Solal K, Pique C, et al. Endomitosis of human megakaryocytes are due to abortive mitosis. *Blood*. 1998;91(10):3711-3723.
34. Musacchio A, Salmon ED. The spindle-assembly checkpoint in space and time. *Nat Rev Mol Cell Biol*. 2007;8(5):379-393.
35. Brito DA, Rieder CL. Mitotic checkpoint slippage in humans occurs via cyclin B destruction in the presence of an active checkpoint. *Curr Biol*. 2006;16(12):1194-1200.
36. Wan L, Tan M, Yang J, et al. APC(Cdc20) suppresses apoptosis through targeting Bim for ubiquitination and destruction. *Dev Cell*. 2014;29(4):377-391.

37. Matthess Y, Raab M, Knecht R, Becker S, Strebhardt K. Sequential Cdk1 and Plk1 phosphorylation of caspase-8 triggers apoptotic cell death during mitosis. *Mol Oncol*. 2014;8(3):596-608.
38. Topham CH, Taylor SS. Mitosis and apoptosis: how is the balance set? *Curr Opin Cell Biol*. 2013;25(6):780-785.
39. Dohner H, Lubbert M, Fiedler W, et al. Randomized, phase 2 trial of low-dose cytarabine with or without volasertib in AML patients not suitable for induction therapy. *Blood*. 2014;124(9):1426-1433.
40. Lin CC, Su WC, Yen CJ, et al. A phase I study of two dosing schedules of volasertib (BI 6727), an intravenous polo-like kinase inhibitor, in patients with advanced solid malignancies. *Br J Cancer*. 2014;110(10):2434-2440.
41. Stadler WM, Vaughn DJ, Sonpavde G, et al. An open-label, single-arm, phase 2 trial of the Polo-like kinase inhibitor volasertib (BI 6727) in patients with locally advanced or metastatic urothelial cancer. *Cancer*. 2014;120(7):976-982.
42. Raab M, Kramer A, Hehlgans S, et al. Mitotic arrest and slippage induced by pharmacological inhibition of Polo-like kinase 1. *Mol Oncol*. 2014.
43. Raab M, Pachl F, Kramer A, et al. Quantitative chemical proteomics reveals a Plk1 inhibitor-compromised cell death pathway in human cells. *Cell Res*. 2014;24(9):1141-1145.

Figure Legends

Figure 1. Defective megakaryocyte maturation in the absence of Plk1. **a)** Bone marrow sections from 8-week-old mice were stained with hematoxylin and eosin (H&E), or antibodies against Plk1 or the Von Willebrand Factor (VWF). Mitotic cells are indicated by arrows. Scale bars, 100 μm (insets, 20 μm). **b)** The quantification of VWF area per cell is shown in the histogram. Horizontal bars indicate the average from >500 cells per condition from at least 3 different animals. ***, $p<0.001$; Student's t-test. **c)** Phosphorylation of histone H3 (pH3) in Plk1-deficient or control megakaryocytes. Scale bars, 100 μm (insets, 20 μm). The quantification of pH3-positive cells is shown in the right histogram. Data are mean ± SD (n=3 mice per genotype). ***, $p<0.001$; Student's t-test. **d)** Representative images of mitotic cells in Plk1-deficient or control mice after staining with hematoxylin and eosin (H&E) or Immunodetection of phosphorylated histone H3 (pH3). Scale bars, 20 μm. **e**) Analysis of nuclear complexity in Plk1-null and control megakaryocytes. Scale bars, 20 μm. In these analyses at least 250 cells from ≥3 different animals per genotype were used. Student's t-test. ***, $p<0.001$.

Figure 2. Defective megakaryocyte ploidy and circulating platelets in *Plk1*(Δ/Δ) mice. **a**) Analysis of DNA content in gated CD41+ cells from the bone marrow of 8-week-old *Plk1*(Δ/Δ) or control mice. The plot is representative of three different animals analyzed per genotype. **b**) Quantification of high-ploidy CD41+ cells (≥16C) in the bone marrow of mice with the indicated genotypes. Data are mean ± SD (n=4 mice per genotype). *, <0.05; **, $p<0.01$; ***, $p<0.001$; Student's t-test. **c)** Number of circulating platelets in

Plk1(Δ/Δ) or control mice. As a comparison the average count is ~100 x 10^9 platelets/L in Cdc20-deficient mice[12]. ***, p<0.001, Student's t-test.

Figure 3. Defective mitotic exit in Plk1-deficient megakaryocytes. **a**) Representative mitotic progression and exit in wild-type megakaryocytes. Cells were transduced with lentiviral vectors expressing GFP-histone H2B (green) and mCherry-Geminin (red). Mitotic entry (time 0) can be monitored by chromosome condensation and pan-cellular staining of geminin. Mitotic exit (1h) is monitored by chromosome decondensation, reformation of nuclear lobules and geminin degradation. **b**) Two independent examples of defective mitotic progression in Plk1-deficient megakaryocytes. Mitotic entry (chromosome condensation and pan-cellular staining of geminin) is shown at time 0 (third frame in the top cell and second frame in the bottom cell). Geminin is slowly degraded 27-32 h after mitotic entry resulting in cell death (top cell) or mitotic exit (bottom) approximately after 37 h. **c**) Representation of cell fate in wild-type and *Plk1*(Δ/Δ) megakaryocytes. Every row represents a single cell. Geminin high phases are shown in red whereas geminin-low phases are in green. Endomitosis is indicated by a purple box and cell death is indicated by a red circle. Mitotic entry (condensation of chromatin and pancellular localization of geminin) is normalized as time 0. **d)** Duration of mitosis (DOM; in hours) in Plk1-deficient or control megakaryocytes. Cdc20-deficient megakaryocytes[12] are used as a control. ***, p<0.001; Student's t-test.

Figure 4. Lack of Plk1 results in defective centrosome maturation and spindle formation in mitotic megakaryocytes. **a)** Reduced polyploidization in Lin$^-$ bone marrow cells three days after stimulation with thrombopoietin (TPO). Data are mean ± SD (n=4 mice per genotype). *<0.05; **, p<0.01; ***, p<0.001; Student's t-test. **b)**

Representative images and quantification of mitotic cells (arrowheads) in these cultures three days after stimulation with TPO. Scale bars, 20 μm (top) and 50 μm (bottom). Data are mean ± SD. At least 250 cells per genotype were scored. ***, $p<0.001$; Student's t-test. **c**) Immunodetection of Plk1 (red) in *Plk1*(lox/lox) and *Plk1*(Δ/Δ) stimulated in vitro with TPO. DAPI (blue) was used to stain DNA. Scale bars, 10 μm. **d**) Quantification of ring structures in the mitotic cells in these cultures. Data are mean ± SD. n=50 (control) or 250 (Plk1- or Cdc20-null) mitotic cells per condition. ***, $p<0.001$; Student's t-test. **e**) Immunodetection of α-tubulin (green) and pericentrin (red) in Plk1-null or control cells treated with the indicated compounds. DAPI (blue) was used to stain DNA. Scale bars, 10 μm. **f)** Quantification of pericentrin median fluorescence intensity (MFI) in these cultures. Horizontal bars indicate averages. ns, not significant; ***, $p<0.001$; Student's t-test.

Figure 5. Accumulation of SAC proteins in the kinetochores of Plk1-deficient megakaryocytes. **a)** Immunodetection of Bub1 (green) and centromeres (ACA, anti-centromeric antibody, magenta) in *Plk1*(Δ/Δ) cells or control cells treated with taxol or the Plk1 inhibitor BI2536. Cdc20-deficient cells were used as a control of SAC-independent mitotic arrest. DAPI (blue) was used to stain DNA. **b)** Immunodetection of Mad2 (red) and centromeres (ACA, anti-centromeric antibody, magenta) in *Plk1*(Δ/Δ) cells or control cells treated with taxol or the Plk1 inhibitor BI2536. Cdc20-deficient cells were used as a control of SAC-independent mitotic arrest. DAPI (blue) was used to stain DNA. Scale bars, 10 μm (insets, 2 μm).

Figure 6. Lack of Plk1 results in a SAC-dependent mitotic arrest. **a)** Representative images of *Plk1*(Δ/Δ) megakaryocytes in the absence or presence of the SAC inhibitor

reversine. Spindles are shown by α-tubulin staining (green) whereas phosphorylation of histone H3 (pH3) is shown in magenta. DAPI (blue) was used to stain DNA. Scale bars, 50 μm (or 20 μm in the two right columns). **b)** Representative images of the indicated cultures in the absence or presence of reversine. Spindles are shown by α-tubulin staining (green) whereas phosphorylation of histone H3 (pH3) is shown in magenta and DAPI (blue) was used to stain DNA. Scale bars, 50 μm (or 20 μm in the bottom raw). In a) and b) arrows indicate curved nuclei around a single tubulin aster. **c)** Mitotic index, as determined by detection of phosphorylated histone H3 (pH3), in Plk1- or Cdc20-deficient cells or control cells treated with taxol or BI2536 in the absence or presence of the Mps1 inhibitor reversine. Data are mean ± SD. n=50 cells per condition. ns, not significant; **, $p<0.01$; ***, $p<0.001$; Student's t-test.

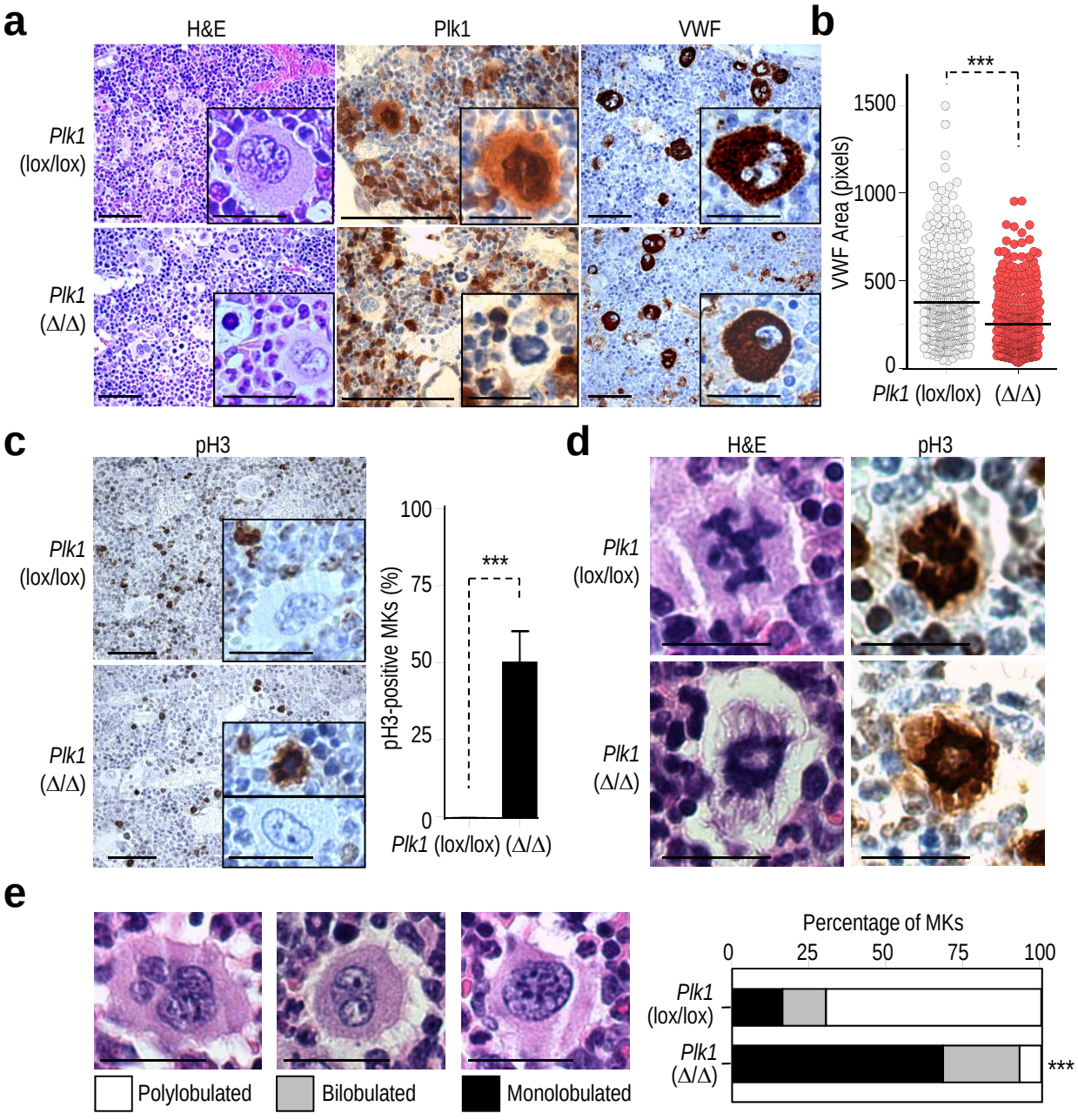
a
H&E
Plk1
VWF
Plk1 (lox/lox)
Plk1 (Δ/Δ)
b
***
VWF Area (pixels)
1500
1000
500
0
Plk1 (lox/lox) (Δ/Δ)
c
pH3
Plk1 (lox/lox)
Plk1 (Δ/Δ)
pH3-positive MKs (%)
100
75
50
25
0
***
Plk1 (lox/lox) (Δ/Δ)
d
H&E
pH3
Plk1 (lox/lox)
Plk1 (Δ/Δ)
e
Polylobulated
Bilobulated
Monolobulated
Percentage of MKs
0
25
50
75
100
Plk1 (lox/lox)
Plk1 (Δ/Δ)
***

Figure 1

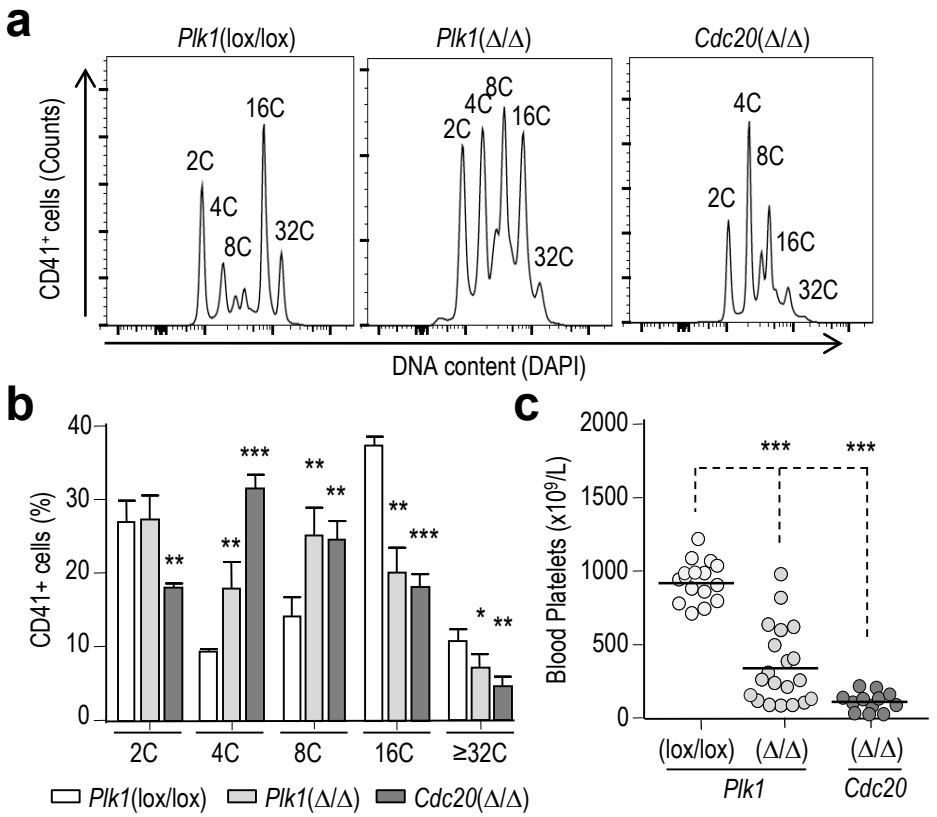
a
Plk1(lox/lox)
Plk1(Δ/Δ)
Cdc20(Δ/Δ)
CD41+ cells (Counts)
2C
4C
8C
16C
32C
DNA content (DAPI)
b
CD41+ cells (%)
40
30
20
10
0
2C
4C
8C
16C
≥32C
Plk1(lox/lox)
Plk1(Δ/Δ)
Cdc20(Δ/Δ)
c
Blood Platelets (x10⁹/L)
2000
1500
1000
500
0
(lox/lox)
(Δ/Δ)
(Δ/Δ)
Plk1
Cdc20

Figure 2

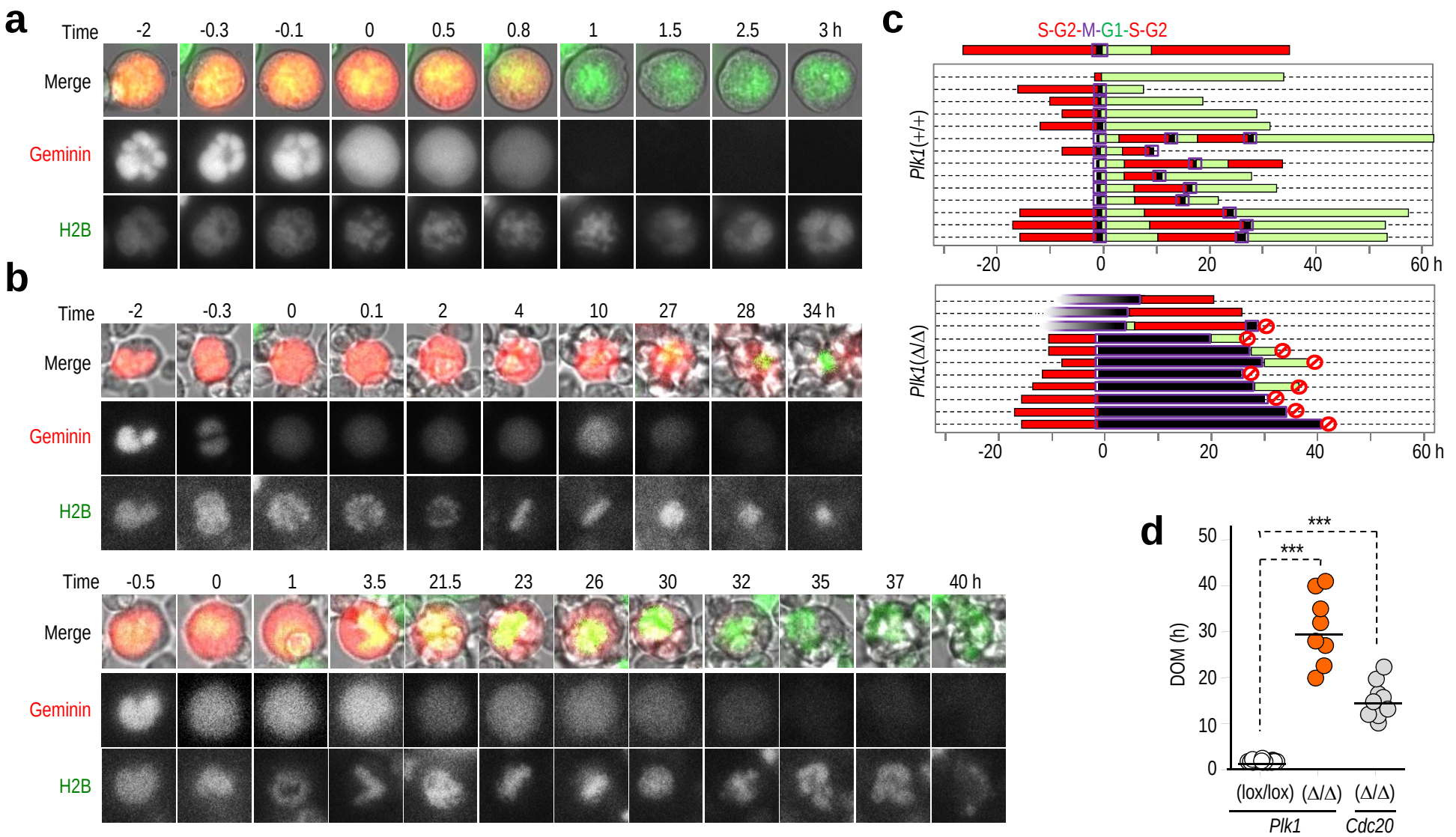
a
Time
-2
-0.3
-0.1
0
0.5
0.8
1
1.5
2.5
3 h
Merge
Geminin
H2B
b
Time
-2
-0.3
0
0.1
2
4
10
27
28
34 h
Merge
Geminin
H2B
Time
-0.5
0
1
3.5
21.5
23
26
30
32
35
37
40 h
Merge
Geminin
H2B
c
S-G2-M-G1-S-G2
Plk1(+/+)
Plk1(Δ/Δ)
-20
0
20
40
60 h
d
DOM (h)
50
40
30
20
10
0
***
***
(lox/lox)
(Δ/Δ)
(Δ/Δ)
Plk1
Cdc20

Figure 3

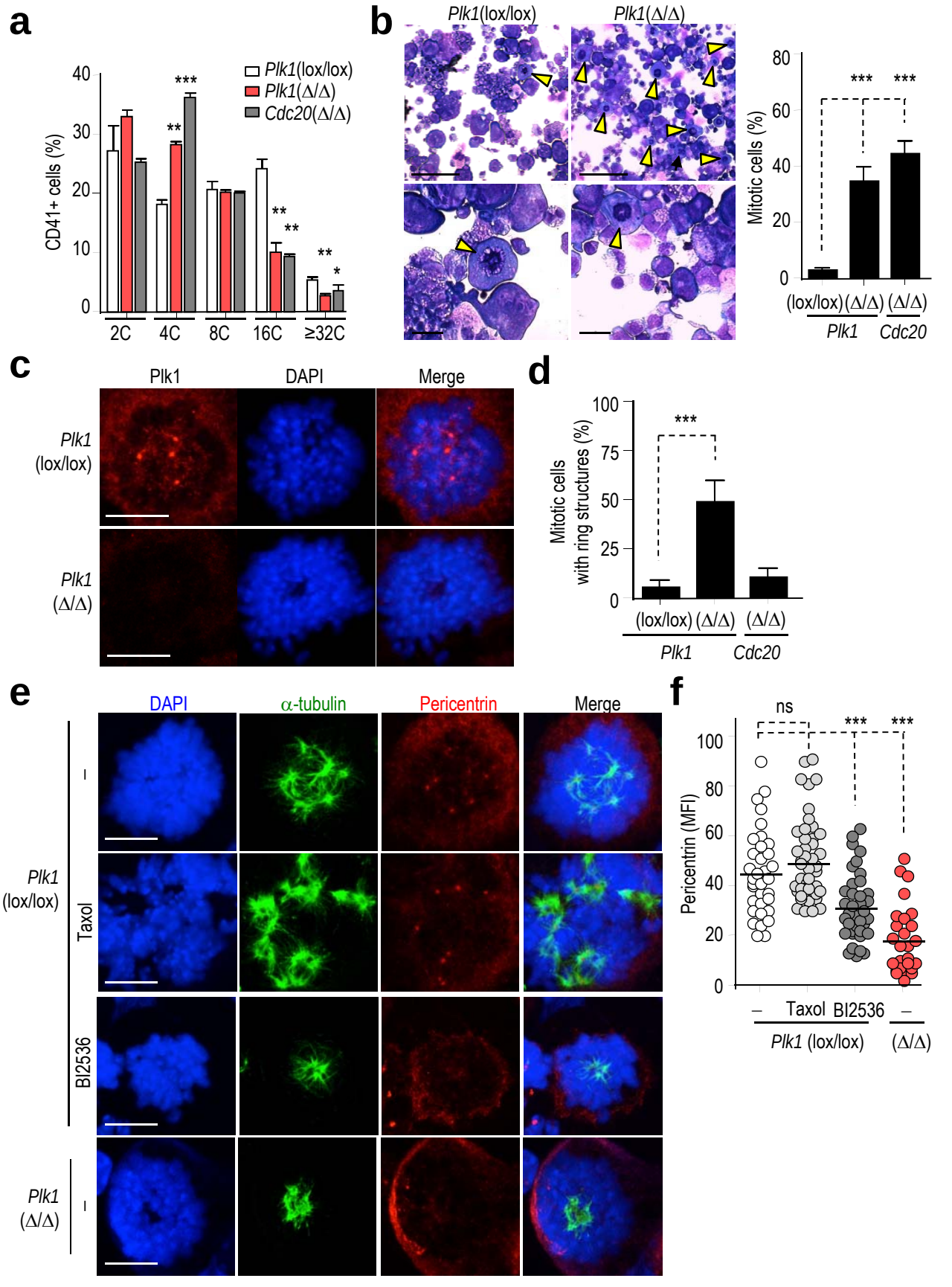
a
Plk1(lox/lox)
Plk1(Δ/Δ)
Cdc20(Δ/Δ)
CD41+ cells (%)
2C
4C
8C
16C
≥32C
b
Plk1(lox/lox)
Plk1(Δ/Δ)
Mitotic cells (%)
(lox/lox)
(Δ/Δ)
(Δ/Δ)
Plk1
Cdc20
c
Plk1
DAPI
Merge
Plk1 (lox/lox)
Plk1 (Δ/Δ)
d
Mitotic cells with ring structures (%)
(lox/lox)
(Δ/Δ)
(Δ/Δ)
Plk1
Cdc20
e
DAPI
α-tubulin
Pericentrin
Merge
Plk1 (lox/lox)
Taxol
BI2536
Plk1 (Δ/Δ)
f
ns
Pericentrin (MFI)
Taxol
BI2536
Plk1 (lox/lox)
(Δ/Δ)

Figure 4

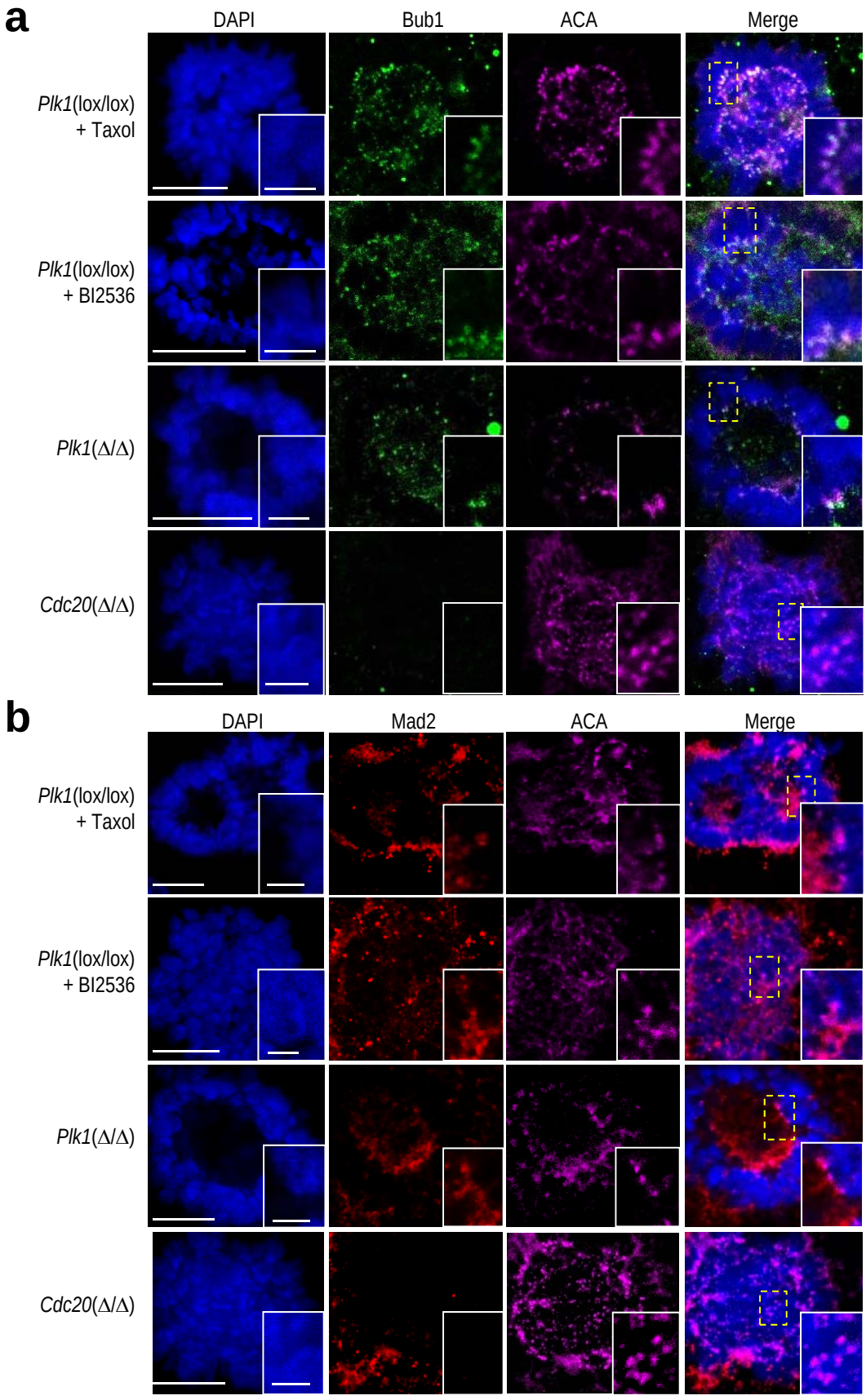
a
DAPI
Bub1
ACA
Merge
Plk1(lox/lox) + Taxol
Plk1(lox/lox) + BI2536
Plk1(Δ/Δ)
Cdc20(Δ/Δ)
b
DAPI
Mad2
ACA
Merge
Plk1(lox/lox) + Taxol
Plk1(lox/lox) + BI2536
Plk1(Δ/Δ)
Cdc20(Δ/Δ)

Figure 5

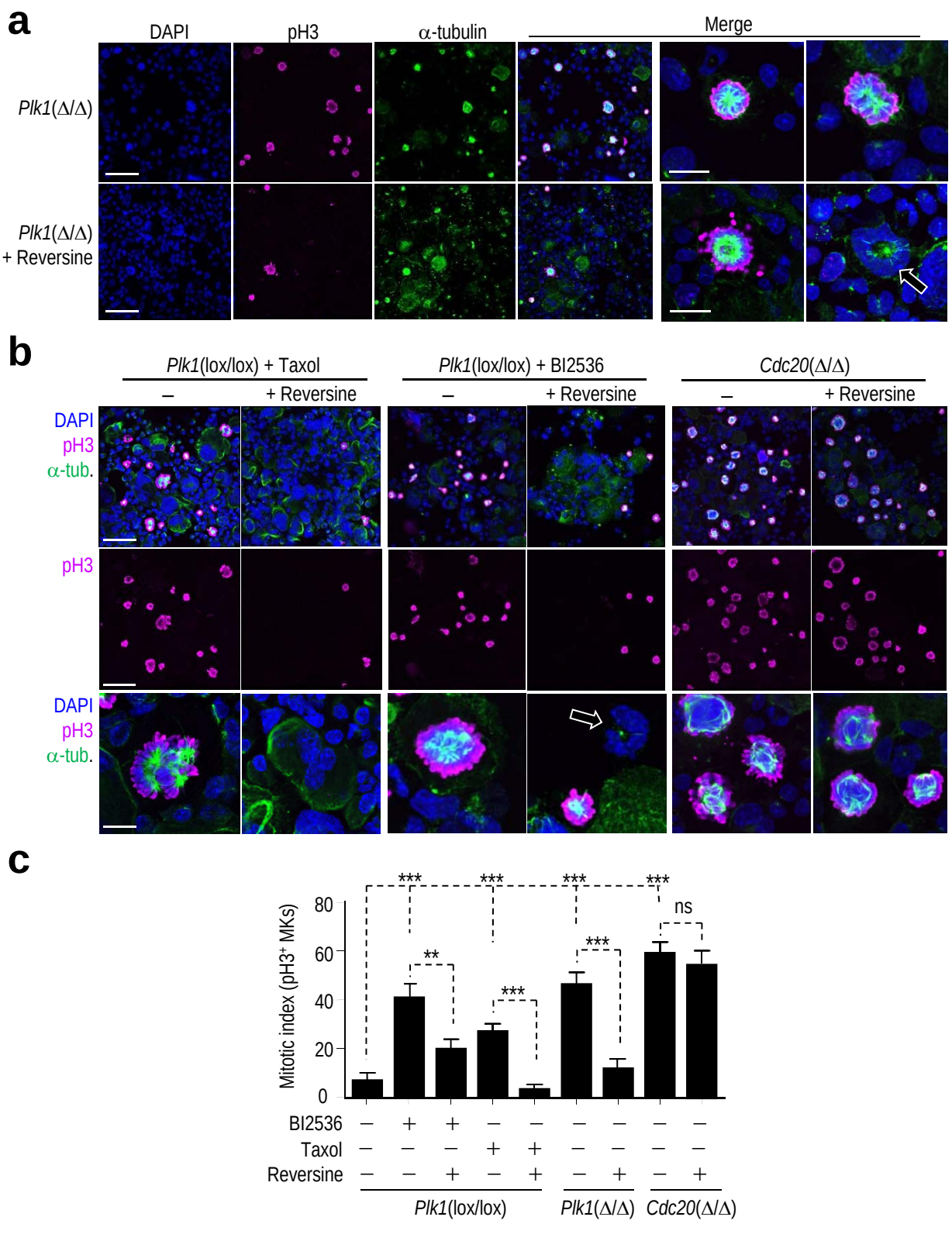
a
DAPI
pH3
α-tubulin
Merge
Plk1(Δ/Δ)
Plk1(Δ/Δ) + Reversine
b
Plk1(lox/lox) + Taxol
Plk1(lox/lox) + BI2536
Cdc20(Δ/Δ)
–
+ Reversine
DAPI pH3 α-tub.
pH3
c
Mitotic index (pH3+ MKs)
80
60
40
20
0
***
**
ns
BI2536
Taxol
Reversine
Plk1(lox/lox)
Plk1(Δ/Δ)
Cdc20(Δ/Δ)

Figure 6